CrossMark

α1-antitrypsin mitigates NLRP3-inflammasome activation in amyloid β_{1-42}-stimulated murine astrocytes

Taraneh Ebrahimi[1], Marcus Rust[1], Sarah Nele Kaiser[1], Alexander Slowik[2], Cordian Beyer[2], Andreas Rembert Koczulla[3], Jörg B. Schulz[1,4], Pardes Habib[1†] and Jan Philipp Bach[1*†]

Abstract

Background: Neuroinflammation has an essential impact on the pathogenesis and progression of Alzheimer's disease (AD). Mostly mediated by microglia and astrocytes, inflammatory processes lead to degeneration of neuronal cells. The NLRP3-inflammasome (NOD-like receptor family, pyrin domain containing 3) is a key component of the innate immune system and its activation results in secretion of the proinflammatory effectors interleukin-1β (IL-1β) and interleukin-18 (IL-18). Under physiological conditions, cytosolic NLRP3-inflammsome is maintained in an inactive form, not able to oligomerize. Amyloid β_{1-42} (Aβ_{1-42}) triggers activation of NLRP3-inflammasome in microglia and astrocytes, inducing oligomerization and thus recruitment of proinflammatory proteases. NLRP3-inflammasome was found highly expressed in human brains diagnosed with AD. Moreover, NLRP3-deficient mice carrying mutations associated with familial AD were partially protected from deficits associated with AD.

The endogenous protease inhibitor α1-antitrypsin (A1AT) is known for its anti-inflammatory and anti-apoptotic properties and thus could serve as therapeutic agent for NLRP3-inhibition. A1AT protects neurons from glutamate-induced toxicity and reduces Aβ_{1-42}-induced inflammation in microglial cells. In this study, we investigated the effect of Aβ_{1-42}-induced NLRP3-inflammasome upregulation in primary murine astrocytes and its regulation by A1AT.

Methods: Primary cortical astrocytes from BALB/c mice were stimulated with Aβ_{1-42} and treated with A1AT. Regulation of NLRP3-inflammasome was examined by immunocytochemistry, PCR, western blot and ELISA. Our studies included an inhibitor of NLRP3 to elucidate direct interactions between A1AT and NLRP3-inflammasome components.

Results: Our study revealed that A1AT reduces Aβ_{1-42}-dependent upregulation of NLRP3 at the mRNA and protein levels. Furthermore, A1AT time-dependently mitigated the expression of caspase 1 and its cleavage product IL-1β in Aβ_{1-42}-stimulated astrocytes.

Conclusion: We conclude that Aβ_{1-42}-stimulation results in an upregulation of NLRP3, caspase 1, and its cleavage products in astrocytes. A1AT time-dependently hampers neuroinflammation by downregulation of Aβ_{1-42}-mediated NLRP3-inflammasome expression and thus may serve as a pharmaceutical opportunity for the treatment of Alzheimer's disease.

Keywords: Neuroinflammation, NLRP3, NALP3, Inflammasome, Alzheimer's disease, Amyloid β, Alpha 1-antitrypsin, Astrocytes

* Correspondence: jbach@ukaachen.de
†P Habib and J P Bach contributed equally to this work.
[1]Department of Neurology, RWTH Aachen University, Aachen, Germany
Full list of author information is available at the end of the article

Ebrahimi *et al. Journal of Neuroinflammation* (2018) 15:282

Page 2 of 15

Background

Alzheimer's disease (AD) is the most common form of dementia with more than 40 million patients affected worldwide [1]. By 2050, the number is expected to quadruple [2]. Age is the most important risk factor [3], because the incidence of AD doubles every 5 years after the age of 65 years [3]. There is no causal treatment so far. To date, almost all biologicals or secretase inhibitors have failed in clinical trials which emphasize the need for further research into novel therapeutic options. Treatment of patients, even with early symptoms, only starts when the disease pathology has progressed and neural tissue has irreversibly been damaged for years. Therefore, current trials focus on patients with prodromal disease signs [4–11].

Following the amyloid hypothesis, accumulation of extracellular $A\beta_{1-42}$-oligomers is one of the earliest and driving factors for pathogenesis of AD [12, 13]. The majority of in vitro studies investigated the effect of $A\beta_{1-42}$ after an incubation time of 24–72 h [14–16]. Current scientific literature reveals less data about a possible damaging effect of $A\beta_{1-42}$-stimulation on the central nervous system (CNS) after short-term stimulation of only a few hours [14].

Besides $A\beta_{1-42}$, AD is mainly characterized by hyperphosphorylation of tau and neuroinflammation mediated by microglia and astrocytes, causing neuronal cell death [17–21]. A key component of the innate immune system is the NOD-like receptor family, pyrin domain-containing 3 (NLRP 3) [22, 23]. Though ubiquitously expressed in CNS, NLRP3 is found highly expressed in Alzheimer's patients' brains [22–24]. Under physiological conditions, an inactive form of NLRP3 is located in the cytoplasm [14, 25]. However, in the absence of activating signals, the NLRP3-inflammasome is not able to oligomerize [25]. After NLRP3-receptors recognize danger signals released by damaged cells and pathogens [26], NLRP3, the adaptor protein ASC (apoptosis-associated speck-like protein containing a CARD) and pro-caspase 1 form a subcellular multiprotein complex, known as NLRP3-inflammasome [22, 23, 27]. Subsequently, pro-caspase 1 is activated by autoproteolysis and catalyzes the cleavage of the precursors pro-IL-1β and pro-IL-18 [27]. Mostly induced by microglia and astrocytes, secretion of pro-inflammatory cytokines IL-1β and IL-18 drives inflammatory responses and causes neuronal damaging [27–29].

Inflammasomes are linked to neurodegenerative diseases: activated NLRP3 was observed in Parkinson's disease in the midbrain and cerebrospinal fluid [30–33]. Furthermore, in an experimental ischemic stroke model, NLRP3-deficiency was protective against ischemic neuronal damage [34].

In a cellular model of Alzheimer's disease, Halle et al. 2008 first described that activation of NLRP3-inflammasome is induced by $A\beta_{1-42}$ in microglia, leading to an overexpression of the pro-inflammatory cytokine IL-1β [14]. Moreover, $A\beta_{1-42}$ activates the NLRP3-inflammasome in astrocytes [35]. Alike microglia, as a part of the CNS immune response, reactive astrocytes surround amyloid deposits and perform phagocytosis [35–37]. Most studies investigated $A\beta_{1-42}$-mediated inflammatory processes in microglia and little is known about inflammasome activation in $A\beta_{1-42}$-stimulated astrocytes [14, 15, 24, 38–40]. Since inflammation occurs as one of the first cellular and molecular responses after cell stress, short-term effects of Aβ-stimulation in astrocytes need further characterization. Aside from cell culture models, also in human models of AD high expression of NLRP3-inflammasome was found. More precise, an upregulation of NLRP3 expression in peripheral monocytes from individuals with AD was identified [16]. Moreover, in frontal cortex and hippocampus lysates from AD patients increased amounts of cleaved caspase 1 were detected [24]. Interestingly, NLRP3 deficient mice carrying genes associated with familial AD were protected from spatial memory deficits [24].

Therefore, a potent inhibition of the NLRP3-inflammasome could be a new therapeutic approach. The protease inhibitor α1-antitrypsin (A1AT) is known for its anti-inflammatory and anti-apoptotic properties in both hepatic and lung cells [41–44]. Conveniently, A1AT is therapeutically used in patients with A1AT-deficiency and therefore well-established as a pharmaceutical agent. Recently, we demonstrated that A1AT also protected neurons from glutamate-induced toxicity [45] and reduced $A\beta_{1-42}$-induced inflammation in microglial cells [15]. In addition, we found that A1AT inhibited calpain and stabilized calcium-homeostasis [15]. This study investigated the regulation of NLRP3-inflammasome by A1AT in $A\beta_{1-42}$-stimulated murine astrocytes. In order to elucidate a direct interaction between A1AT and the NLRP3-inflammasome, we have included an inhibitor of NLRP3. MCC950 is a highly potent and specific inhibitor of NLRP3, without affecting AIM2, NLRC4, or NLRP4 [46–49]. Recent data revealed that MCC950 stimulated Aβ-phagocytosis in vitro, and reduced Aβ-accumulation in a mouse model of AD, which was associated with improved cognitive function [50].

Methods

Primary cortical murine astrocyte culture

Postnatal (P0 to P2) cortical astrocyte culture preparation from BALB/c mice (Charles River) was performed as previously described by Habib et al. 2014 [51]. Preparation was conducted in accordance with animal welfare policy of University Hospital Aachen and the government of the State of North Rhine-Westphalia, Germany (no. 84.02.04.2015.A292). Briefly, after brain dissection meninges and blood vessels were removed, cortex was isolated, homogenized, and dissolved in Dulbecco's

Ebrahimi *et al. Journal of Neuroinflammation* (2018) 15:282

Page 3 of 15

phosphate-buffered saline (DPBS, Life Technologies, USA) containing 1% (*v/v*) trypsin and 0.02% (*v/v*) EDTA. The cell suspension was filtered through a 50 μm nylon mesh. After centrifugation (1400 rpm, 5 min), pellets were re-suspended in Gibco™ Dulbeccos's modified Eagle medium (DMEM, Life Technologies, USA) and seeded on flasks in DMEM with additional 10% fetal bovine serum (FBS, PAA, Austria) and 0.5% penicillin-streptomycin (Invitrogen, USA). All flasks and plates were coated by poly-L-ornithine (PLO, Sigma-Aldrich, Germany) prior to cell seeding. Cells were kept in a humidified incubator at 37 °C and 5% CO_2. After cell confluence was about 80%, flasks were shaken for 2 h (150 rpm, 37 °C) to remove microglia and oligodendrocytes from astrocytes. Additionally, before each subcultivation the 2 h machine shaking was repeated, the contaminating cells were transferred to the medium and then removed.

For subcultivation, cells were trypsinized with 2.5% (*v/v*) trypsin diluted in PBS/EDTA and seeded on new flasks in a 1:3 ratio. Medium was refreshed every second day. Subcultivation was performed when cells reached a confluence of about 80%. At passage 2, astrocytes were seeded on experimental plates 48 h prior to stimulation. 24 h before stimulation medium was changed to phenol red-free Gibco™ Roswell Park Memorial Institute (RPMI 1640, Life Technologies, USA) with additional 5% FBS and 0.5% penicillin-streptomycin (Fig. 1a).

Astrocyte culture purity was examined by immunocytochemistry (ICC) using anti-GFAP-antibody (glial fibrillary acidic protein), anti-Iba1-antibody (ionized calcium binding adaptor molecule 1), anti-Olig2-antibody (oligodendrocyte transcription factor 2) and Hoechst (33342, Trihydrochloride, Trihydrate, Invitrogen, USA) for nucleus staining. A detailed list of antibodies used for ICC is illustrated in Table 1. The average of astrocyte purity was 95%, less than 5% of the cells were microglia, under 0.5% of the cells remained undefined (Additional file 1: Figure S2B).

Preparation of A1AT, amyloid β$_{1-42}$, LPS, and MCC950

A1AT originated from Prolastin (Grifols, Barcelona, Spain). 1000 mg of the powder were dissolved in 25 mL ultrapure water to obtain a concentration of 40 mg/mL. The solution was aliquoted and stored at − 80 °C.

To generate Amyloid β$_{1-42}$ oligomers, we used the procedure described by Kayed et al. [52] and Gold et al. [15]. Briefly, 300 μg Aβ$_{1-42}$ (Bachem, Bubendorf, Switzerland) were dissolved in 90 μL hexafluoroisopropanol, 210 μL ultrapure water and diluted with 900 μL 100 mM NaCl, 50 mM Tris (pH 7.4). The solution was stirred for 48 h on a magnetic stirrer at room temperature. Next, the tube was weighed again, and weight difference was adjusted with 100 mM NaCl 50 mM Tris (pH 7.4). The Aβ$_{1-42}$ concentration of this solution was 56 mM. After centrifugation (16,000×*g*, 10 min), the supernatant was used for cell culture experiments. A negative control containing all ingredients but Aβ$_{1-42}$ was established to evaluate possible solvent effects on astrocytes. Lipopolysaccharides (LPS) from *Escherichia coli* (Sigma-Aldrich, Germany) were used at a concentration of 1 μg/mL, as an extra stimulus for maximum cell stimulation. Stimulation time of all reagents was 3 h and 6 h. In order to reveal the short-term inflammasome regulation after Aβ$_{1-42}$ and to understand the mechanism of early inflammation in AD, we decided for short term stimulation of cells.
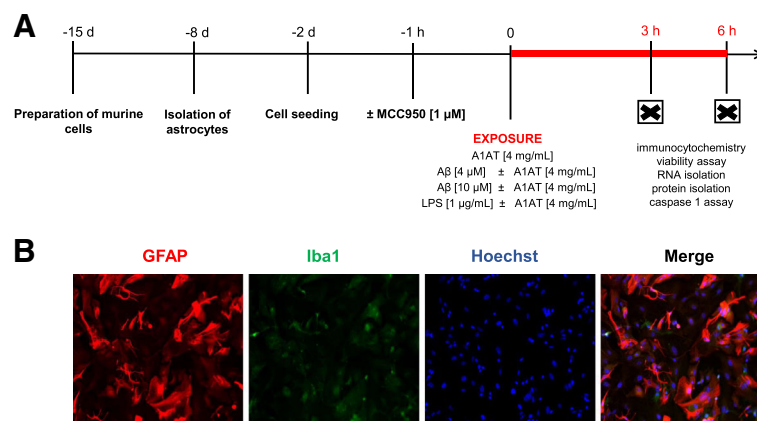

Fig. 1 Experimental setting. **a** Cortices from BALB/c mice were prepared and seeded on flasks 2 weeks prior to stimulation. After a week, when cell confluence was about 80%, flasks were shaken to remove microglia and oligodendrocytes from astrocytes. At passage 2, astrocytes were seeded on experimental plates 48 h prior to stimulation. After short-term stimulation (3 h/ 6 h) with two concentrations of Aβ$_{1-42}$ (4, 10 μM) or LPS (1 μg/mL) and treatment with A1AT (4 mg/mL) immunocytochemistry, viability assays, caspase 1 assay, RNA and protein isolation were performed. For our control experiments, pretreatment with MCC950 (1 μM) was performed 1 h prior to stimulation. **b** Astrocyte purity was assessed by ICC using GFAP and Iba1 combined with Hoechst for DNA staining

Ebrahimi *et al. Journal of Neuroinflammation* (2018) 15:282

Page 4 of 15

Table 1 Antibodies for immunocytochemistry

Antibody	Company	Order no.	Host	Dilution
Anti-goat 488	Life Technologies, USA	A11055	Donkey	1:500
Anti-goat 594	Life Technologies, USA	A11058	Donkey	1:500
Anti-mouse 488	Life Technologies, USA	A21202	Donkey	1:500
Anti-mouse 594	Life Technologies, USA	A21203	Donkey	1:500
Anti-rabbit 488	Life Technologies, USA	A21206	Donkey	1:500
Anti-rabbit 594	Life Technologies, USA	A21207	Donkey	1:500
GFAP	EnCor Biotechnology, USA	RPCA-GFAP	Rabbit	1:1000
Iba 1	Abcam, UK	ab107159	Goat	1:200
Iba 1	Millipore, USA	MABN92	Mouse	1:600
Iba 1	Wako, Japan	019–19,741	Rabbit	1:1000
NLRP3	Adipogen, USA	AG-20B-0014	Mouse	1:333
Olig2	Millipore, USA	MABN50	Mouse	1:1000
Olig2	Millipore, USA	AB9610	Rabbit	1:500

Primary and secondary antibodies used for immunocytochemical staining are listed

MCC950 (Adipogen, USA) was diluted in DMSO (dimethylsulfoxid, Sigma-Aldrich, Germany) and used in a concentration of 1 μM. MCC950 incubated 1 h before further treatment, according to previous studies by Coll et al. [46]. Then, treatment with A1AT, Amyloid β_{1-42}, and LPS was performed for 3 h and 6 h.

Cells were kept in the incubator at 37 °C and 5% CO_2.

Dose-dependency studies

A dose-dependency study with increasing concentrations of A1AT [1, 2, 4, 8, 10, and 12 mg/mL] and $A\beta_{1-42}$ [1, 2, 4, 8, 10, and 12 μM] was performed to determine the sublethal concentration for primary astrocytes. Lactate dehydrogenase (LDH) and Cell Titer-Blue (CTB) assay were used to assess cell viability after 3 h stimulation.

Cell viability

LDH-release

CytoTox 96® Non-Radioactive Cytotoxicity Assay (Promega, USA) was performed according to the manufacturer's protocol to measure release of lactate dehydrogenase (LDH) as a marker of cellular viability. Astrocytes were seeded on a 96-well plate 48 h prior to stimulation and were finally stimulated with $A\beta_{1-42}$ or LPS, and treated with A1AT. After 3 h/6 h incubation time, 50 μL of each well was transferred to a fresh 96-well plate. In addition to a no-treatment-cell control, a no-cell control, one positive control containing LDH and a control containing astrocytes lysed with Triton X-100 were used. CytoTox 96® Reagent (Promega, USA) was added to each well, and the absorbance was recorded at 490 nm by Infinite® M200 (Tecan, Switzerland). Data are presented as percentage of maximum LDH release (100%), which was determined by astrocytes lysed with 1% Triton X-100.

CTB assay

CellTiter-Blue® Cell Viability Assay (Promega, USA) was performed according to manufacturer's protocol to assess metabolic activity of the cells. Astrocytes were seeded on a 96-well plate 48 h prior to stimulation and finally stimulated with $A\beta_{1-42}$ or LPS and treated with A1AT. After 3 h and 6 h incubation time, CellTiter-Blue® Reagent (Promega, USA) was added to each well. After 2.5–3 h, a color switch (reduction of resazurin) was observed and fluorescence was recorded at $560_{Ex}/590_{Em}$ by Infinite® M200 (Tecan, Switzerland).

Semi-quantitative and quantitative real-time PCR

After 3 h/6 h of stimulation, medium was removed and peqGOLD TriFast™ (Peqlab, Germany) was added to cells. RNA was isolated using phenol-chloroform extraction method as previously described [53]. Afterwards, RNA concentration was measured by NanoDrop® ND-1000 (Thermo Fisher Scientific, USA). RNA purity was examined using 260/280 ratio, which was at 2.0 ± 0.1. Samples were diluted with ultrapure water to attain same RNA concentration in each sample. For DNA transcription, samples were transcribed by moloney murine leukemia virus (M-MLV) reverse transcriptase (Invitrogen™, USA) using random primer (Invitrogen™, USA). Semi-quantitative PCR with 30–32 cycles was performed to assess cDNA transcription success, starting with reference genes primer HPRT (hypoxanthine phosphoribosyltransferase 1), GAPDH (glycerinaldehyd-3-phosphate-dehydrogenase), and Hsp90 (heat shock protein 90). Table 2 contains all primers used for PCR. Positive control contained mouse cortex and negative control contained ultrapure water. A Thermocycler Mastercycler ep gradient S (Eppendorf, Germany) was used with the following settings: 3 min at 95 °C, 40 s at 95 °C, 40 s at respective annealing temperature

Ebrahimi et al. Journal of Neuroinflammation (2018) 15:282

Page 5 of 15

Table 2 Primers for PCR

Primer	Sequence	Bp	AT
ASC	Forward: CTTGTCAGGGGATGAACTCAAAA Reverse: GCCATACGACTCCAGATAGTAGC	154	60
Casp1	Forward: CCGTGGAGAGAAACAAGGAGT Reverse: CCCCTGACAGGATGTCTCCA	180	62
GAPDH	Forward: TGTGTCCGTCGTGGATCTGA Reverse: CCTGCTTCACCACCTTCTTGA	77	65
HPRT	Forward: GCTGGTGAAAAGGACCTCT Reverse: CACAGGACTAGAACACCTGC	249	61
Hsp90	Forward: TACTACTACTCGGCTTTCCCGT Reverse: TCGAATCTTGTCCAGGGCATC	192	64
IL-1β	Forward: CAGCTCATATGGGTCCGACA Reverse: CTGTGTCTTTCCCGTGGACC	251	61
IL-18	Forward: SGCCTGTGTTCGAGGATATGACT Reverse: CCTTCACAGAGAGGGTCACAG	122	62
NLRP3	Forward: CCTGGGGGACTTTGGAATCA Reverse: GATCCTGACAACACGCGGA	113	65

List of primers, respective sequences, base pairs (bp) and annealing temperature in °C (AT) used for sq-PCR and q-RT-PCR

(Table 2), and 45 s at 72 °C, 45 s at 72 °C. Nucleic acids were detected after application on 3% agarose gel containing Midori Green Advance (Biozym, Germany) for DNA staining and electrophoresis (25 min, 125 V constant, 400 mA). Gels were then photographed in E-box VX2 (Peqlab, Germany).

For quantitative real-time PCR, a dilution series containing all samples was established, starting from 100% with dilution factor 2. Then, samples were diluted 1:10 with ultrapure water. Master mixture included SensiMix™ SYBR and Fluorescein (Bioline, USA), ultrapure water and primer (Table 2). CFX Connect™ Real-Time PCR Detection System (Bio-Rad, USA) was used. The following settings were adjusted: 10 min at 95 °C, 15 s at 95 °C, 30 s at respective annealing temperature (40 cycles), 30 s at 72 °C, and 5 s at 72 °C. The software quantified DNA products by melting curve analysis. An addition gel electrophoresis was performed to control the size of the amplified DNA products. First, the expression of reference genes was measured. All following target gene expressions were normalized to reference genes HPRT, GAPDH, and Hsp90. Using the qbase+ software (Biogazelle, Belgium), the relative quantification was calculated by the ΔΔCt-method and data were expressed as relative amount of the three housekeeping genes, respectively, by using the multiple reference gene normalization method. Untreated cell controls were set to 1.

Immunocytochemistry

Immunocytochemistry (ICC) was performed as previously described by Habib et al. 2014 [51]. Astrocytes were seeded on cover slips on a 24-well plate. After stimulation, cells were fixed with 3.7% paraformaldehyde, lysed with Triton X-100, blocked with blocking buffer, and incubated with primary antibody. A negative control was established by incubating the cover slip only with blocking buffer without primary antibody. On the next day, the secondary antibody was applied and incubated for 2 h. After washing the cover slips, nuclei were stained by Hoechst (33342, Trihydrochloride, Trihydrate, Invitrogen, USA). A detailed list of antibodies used for ICC can be found in Table 1. Fluorescence images were taken with Leica DM6000 B (Leica Microsystems, Germany). For each experiment, the identical microscope settings were selected. Fluorescence intensity was measured using ImageJ (USA),

Western blot

Samples were generated from cell lysate and supernatant. Pierce™ BCA Protein Assay Kit (Thermo Fisher Scientific, USA) was used according to manufacturer's protocol to measure protein concentration. The absorbance was recorded at 562 nm by Tecan Infinite® M200 reader (Tecan, Switzerland). Western blot was performed as previously described by Dang et al. 2011 [54, 55]. Briefly, after astrocytes were stimulated for 3 h/ 6 h, the lysis and extraction buffer as well as protease inhibitors were added. The buffer consists of 10 mM HEPES (PromoCell, Germany), 1.5 mM MgCl2 (Sigma-Aldrich, Germany), 10 mM KCl, 0.5 mM DTT, and 0.05% NP-40 (pH = 7.9.).

Samples were heated for 5 min at 95 °C, loaded on gels, and electrophoresis was performed (10 min at 80 V, 1 h at 140 V). PVDF membranes (Trans-Blot® Turbo™ RTA Mini PVDF Transfer Kit, Bio-Rad, USA) were activated with methanol, and then blotting was performed by Trans-Blot® Turbo™ Transfer System (Bio-Rad, USA) (22 min, 14 V). Blotting success was verified by incubating the membrane with methanol and Ponceau S. The membrane was incubated with the primary antibody overnight; on the next day, the secondary antibody was added after washing the membrane. Table 3 reveals the antibodies used. Chemiluminescence detection system was performed using Pierce™ ECL Western Blotting Substrate (Thermo Fisher Scientific, USA). Densitometric analysis was performed using ImageJ Software (USA).

ELISA

Samples were generated from supernatant. Pierce™ BCA Protein Assay Kit (Thermo Fisher Scientific, USA) was used according to manufacturer's protocol to measure protein concentration. The absorbance was recorded at 562 nm by Tecan Infinite® M200 reader (Tecan, Switzerland). Murine IL-1β Standard ABTS ELISA (PeproTech, USA) was performed according to manufacturer's protocol. Capture antibody was incubated on a 96-well plate overnight. Wells were blocked for 1 h then incubated overnight with standard and samples in triplicate. Next, detection antibody was incubated for 2 h. Avidin-HRP conjugate was incubated for 30 min, afterwards ABTS was added. The color

Ebrahimi *et al. Journal of Neuroinflammation* (2018) 15:282

Page 6 of 15

Table 3 Antibodies for western blotting

Antibody	Company	Order no.	Host	Dilution
Anti-mouse	Sigma-Aldrich, Germany	A4416	Goat	1:4000
Anti-rabbit	Bio-Rad, USA	170–6515	Goat	1:5000
ASC (N15)-R	Santa Cruz, USA	sc-22514-R	Rabbit	1:1000
Caspase 1	Adipogen	20B0042C100	Mouse	1:1000
Caspase 1 p10	Santa Cruz, USA	sc-514	Rabbit	1:1000
Caspase 1 p20	Bioss	bs-6368R	Rabbit	1:500
IL-1β	Abcam, UK	ab9722	Rabbit	1:1000
IL-1β	Cell Signaling Technology, USA	12242S	Mouse	1:1000
IL-18	Abcam, UK	Ab71495	Rabbit	1:1000
IL-18	Santa Cruz, USA	sc-7954	Rabbit	1:1000
NLRP3	Bioss, USA	bs-10021R	Rabbit	1:1000
β-actin	Santa Cruz, USA	sc-47,778	Mouse	1:5000

List of primary and secondary antibodies used for western blotting. Antibodies were diluted in 5% milk

development was recorded at 405 nm by Tecan Infinite® M200 reader (Tecan, Switzerland).

Caspase 1 assay

FAM-FLICA® Caspase-1 Assay Kit (ImmunoChemistry Technologies, USA) was performed according to the manufacturer's protocol to detect caspase 1 activity after 3 h and 6 h stimulation time. FLICA was incubated for 1 h at 37 °C. Hoechst 33342 (1:10000) was used for nuclear staining, cells then were fixed with 3.7% paraformaldehyde. Fluorescence images were taken with Leica DM6000 B (Leica Microsystems, Germany); for each experiment, the exact same microscope settings were adjusted. The number of caspase 1 active cells was counted and set in relation to the total amount of counted astrocytes per well. For each treatment group, 100 cells/well in 5 wells were counted.

Data analysis

All experiments were performed at least three times in triplicate. All data are presented as arithmetic mean ± standard deviation of the mean. Prior to the analysis the residuals of data were tested for normal distribution with the Shapiro-Wilk normality test using JMP® (Version 10, SAS Institute Inc., Cary, NC, USA, 1989–2007). Secondly, equal variance was tested with the Bartlett test. In case that one of these tests was significant, a Box-Cox transformation was performed, and the test for normality and equal variance were repeated with the new calculated values. Finally, a one-way ANOVA was applied followed by the Tukey-HSD post-hoc test for intergroup differences. When transformation of data failed to convert non-normal into normal distributed data, rank data were calculated and used for one-way ANOVA analysis, which results in the Kruskal-Wallis non-parametric analysis followed by the Tukey-HSD post-hoc test. Statistical

significance was set at p value ≤ 0.05 ($*^{/a} \leq 0.05$, $**^{/aa} \leq 0.01$, $***^{/aaa} \leq 0.001$).

Results

After primary astrocytes were stimulated according to work flow (Fig. 1a), culture purity of 95% astrocytes on average was examined by ICC, less than 5% of the remaining cells were microglia (Fig. 1b, Additional file 2: Figure S1 and Additional file 1: Figure S2).

Amyloid β$_{1-42}$ had a dose-dependent cytotoxic effect on astrocytes

First, we incubated astrocytes with Aβ$_{1-42}$ for 3 h to assess the short-term effect on cell viability. A concentration range of frequently used doses between 1 μM and 12 μM was selected [14, 15]. Aβ$_{1-42}$ induced a concentration-depended release of LDH into the medium, reaching 50% release and a significant difference compared to the control condition at a concentration of 12 μM (Additional file 3: Figure S3A). In comparison, the stimulation with LPS (1 μg/mL) led to a LDH-release of about 60%. The metabolic activity of Aβ$_{1-42}$-stimulated primary astrocytes (Cell Titer-Blue-assay) revealed no significant dose-dependent differences (Additional file 4: Figure S4A). To rule out cytotoxic effects, the further studies were performed with sublethal doses of Aβ$_{1-42}$ at 4 μM and 10 μM.

To examine a possible cytotoxic effect of A1AT, dose-dependency studies were performed. 3 h incubation of astrocytes with increasing concentrations of 1 mg/mL to 12 mg/mL of A1AT did not affect LDH release (Additional file 3: Figure S3B), also CTB assay showed no influence on metabolic activity of astrocytes (Additional file 4: Figure S4B).

Moreover, co-exposure of astrocytes with Aβ$_{1-42}$ (4 μM and 10 μM) and A1AT (1 mg/mL) had no impact on LDH release (Fig. 2a, c, Additional file 3: Figure S3C)
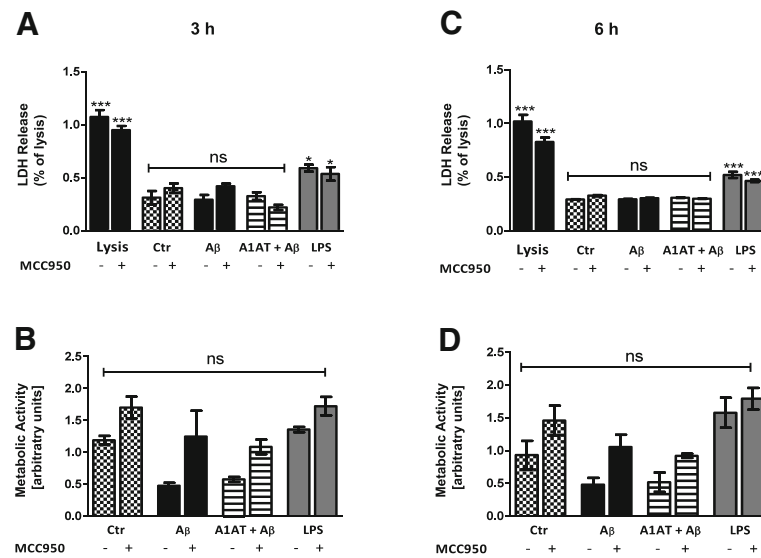
Fig. 2 Effect of $A\beta_{1-42}$ stimulation and A1AT treatment ± MCC950 on cell viability at 3 h and 6 h. Treatment with $A\beta_{1-42}$ [4 μM], A1AT [4 mg/mL], and MCC950 [1 μM] did not affect LDH-release at 3 h and 6 h stimulation, whereas LPS-stimulation [1 μg/mL] significantly increased LDH-release (**a, c**). Cell lysis defined maximal (100%; 1.0) release of LDH. MTT-assay (**b, d**) revealed a trend towards decrease in cell metabolism after 3 h and 6 h $A\beta_{1-42}$-stimulation, which was not significant. Treatment with MCC950 led to an increase of cell metabolism in each treatment group at 3 h and 6 h, which was not significant. */a $p < 0.05$; **/aa $p < 0.01$; ***/aaa $p < 0.001$, ns not significant compared to untreated cell control (ctr)

or cell metabolism (Fig. 2b, d, Additional file 4: Figure S4C). In contrast, A1AT exposure of LPS-stimulated astrocytes significantly reduced LDH release (Additional file 3: Figure S3C).

A1AT prevented $A\beta_{1-42}$-induced upregulation of NLRP3 mRNA and protein

We next evaluated the expression of NLRP3 in the given experimental settings. Stimulation of astrocytes with $A\beta_{1-42}$-oligomers significantly increased NLRP3 mRNA-expression by three-fold ($A\beta_{1-42}$, 4 μM) or four-fold ($A\beta_{1-42}$, 10 μM) in comparison to untreated controls (Fig. 3a, Fig. 4c, d). Co-treatment with 4 mg/mL A1AT almost completely blocked this increase (Fig. 3a, Fig. 4c, d). Western blot analysis revealed a significant higher protein expression of NLRP3 in $A\beta_{1-42}$-stimulated astrocytes compared to untreated controls (Fig. 3b, c, Fig. 4a, b). Co-treatment with A1AT significantly prevented this increase in NLRP3 protein expression (Fig. 3c, Fig. 4a, b). These results were confirmed by ICC. Staining with GFAP-, NLRP3-antibody and Hoechst revealed significantly higher fluorescence intensity of NLRP3-stained astrocytes stimulated with 10 μM of $A\beta_{1-42}$ (Fig. 3d, e, microscope settings were identical for each experiment). Fluorescence intensity of $A\beta_{1-42}$-stimulated cells significantly declined with co-treatment by A1AT (Fig. 3e).

To exclude that NLRP3-upregulation was due to microglia contamination, ICC-staining using Iba1- and NLRP3-antibody was performed (Additional file 5: Figure S5). Indeed, NLRP3 was expressed by the few present microglia. But as Additional file 1: Figure S2 and Additional file 5: Figure S5 show, the amount of microglia was so low, that their impact on NLRP3-expression is negligible.

$A\beta_{1-42}$-stimulation and A1AT-treatment did not regulate ASC expression

The NLRP3-inflammasome consists of active NLRP3 (LRR, NACHT, PYD, CARD) as well as the adaptor protein ASC and pro-caspase 1. In primary astrocytes, treatment with 4 μM or 10 μM $A\beta_{1-42}$ or 4 mg/mL A1AT did not result in changes of ASC mRNA or protein expression at 3 h and 6 h stimulation time (Fig. 5).

A1AT abrogated $A\beta_{1-42}$-induced upregulation of caspase 1 and the pro-inflammatory cytokine IL-1β

Next, we analyzed caspase 1, IL-1β and IL-18 expression. Whereas 3 h treatment of primary astrocytes with 4 μM of $A\beta_{1-42}$ did not result in an increase of caspase 1 mRNA expression, treatment with 10 μM of $A\beta_{1-42}$ led to a significant increase of caspase 1 mRNA expression (Fig. 6a, Additional file 6: Figure S6A). Co-treatment with 4 mg/mL A1AT blocked the increase of caspase 1 expression significantly (Additional file 6: Figure S6A). Repeating this experiment, this time performing a 6-h stimulation, revealed that $A\beta_{1-42}$ significantly increased mRNA levels of caspase 1 in astrocytes (Fig. 6b). Co-treatment with A1AT blocked this increase in caspase 1 mRNA (Fig. 6b).
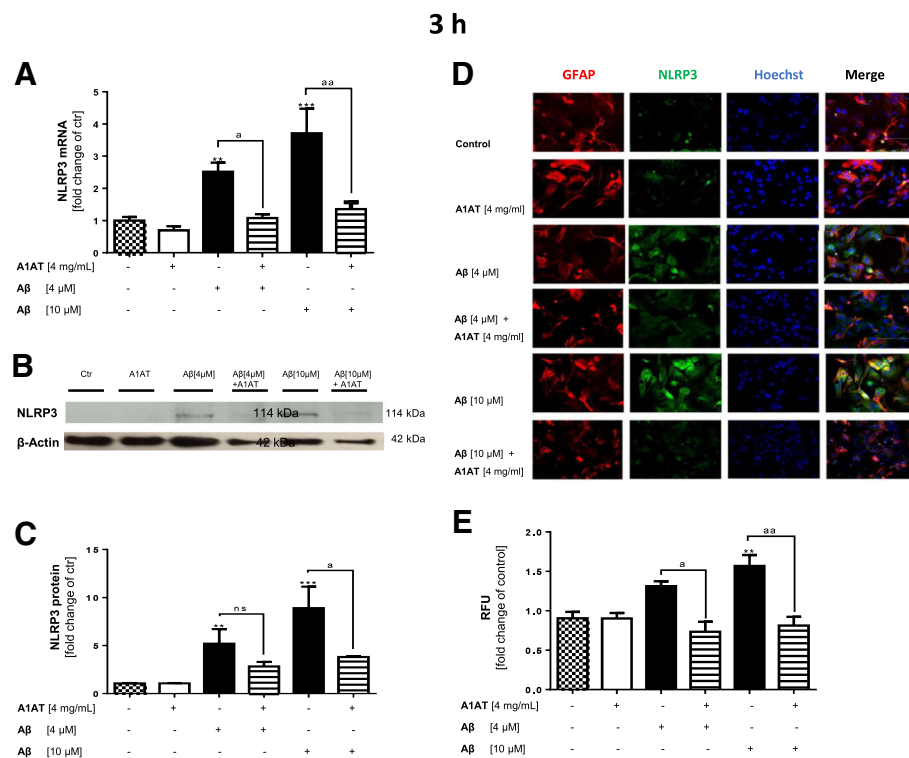
Ebrahimi et al. Journal of Neuroinflammation (2018) 15:282

Page 8 of 15

Fig. 3 Treatment with A1AT abrogated $A\beta_{1-42}$-induced upregulation of NLRP3 mRNA and protein in primary astrocytes. **a** As quantified by RT-PCR treatment with 4 μM and 10 μM of $A\beta_{1-42}$ significantly increased mRNA levels of NLRP3 in astrocytes. In addition, co-treatment with 4 mg/mL of A1AT blocked this increase in NLRP3 mRNA expression significantly. Data of $n = 6$ in triplicate represent mean ± SD. **b–c** Densitometric analysis of western blots confirmed an $A\beta_{1-42}$-induced significant increase of NLRP3 protein levels at 3 h. Treatment with 4 mg/mL of A1AT significantly attenuated this increase at 10 μM $A\beta_{1-42}$. Data of $n = 3$ in triplicate represent mean ± SD. **d–e** Astrocytes treated with 10 μM of $A\beta_{1-42}$ showed a significant increase of NLRP3-fluorescence intensity, whereas co-treatment with A1AT significantly reduced NLRP3-expression. Fluorescence images of each experiment were taken using the exact same microscope settings and fluorescence intensity was measured by ImageJ (USA). Data of $n = 4$ in triplicate represent mean ± SD. */a$p < 0.05$; **/aa$p < 0.01$; ***/aaa$p < 0.001$, ns not significant compared to untreated cell control (ctr)

FAM-FLICA® Caspase-1 Assay, measuring active caspase-1 enzyme, showed that treatment with $A\beta_{1-42}$ significantly induced the number of caspase 1 positive cells (Fig. 7). Co-treatment with 4 mg/mL of A1AT significantly blocked this increase of caspase 1-positive cells (Fig. 7).

In the next step, pro-inflammatory cytokines cleaved by caspase 1 were assessed. Stimulation of astrocytes with 4 μM and 10 μM of $A\beta_{1-42}$ increased mRNA expression of IL-1β (Fig. 8a, b, Additional file 6: Figure S6B). Co-treatment with A1AT significantly reduced mRNA expression of IL-1β (Fig. 8a, b, Additional file 6: Fig. 6b). In contrast, IL-18 gene expression was not affected by either of the treatments at 3 h stimulation time (Fig. 8c, Additional file 6: Figure S6C). However, 6 h stimulation with $A\beta_{1-42}$ significantly increased mRNA levels of IL-18 in astrocytes, but A1AT did not block this effect (Fig. 8d).

Furthermore, western blot revealed a significant upregulation of the IL-1β-precursor in $A\beta_{1-42}$-treated cells (Fig. 9a, b). Co-treatment with A1AT blocked the effect (Fig. 9a, b). Analysis of IL-1β protein by ELISA revealed a similar effect of increased levels after $A\beta_{1-}$ $_{42}$-stimulation, which was significant at 6 h, but not at 3 h (9C-D). A1AT-treatment significantly prevented this increase time-dependently after 6 h stimulation (Fig. 9d).

MCC950 reduced caspase 1 activity and IL-1β protein expression

In order to elucidate a direct interaction between A1AT and the NLRP3-inflammasome, all studies were repeated including MCC950—a selective inhibitor of NLRP3. MCC950 had no impact on cell viability (Fig. 2a, c), but led to an increase of cell metabolism in each treatment group at 3 h and 6 h, though not significant (Fig. 2b, d). In western blot, MCC950 did not change protein levels of NLRP3 (Fig. 4a, b). Treatment with MCC950 did not alter gene expression of NLRP3, ASC, caspase 1, IL-1β, and IL-18 (Figs. 4c, d, 5E–F, 6a, b, 8a, d).

MCC950 significantly mitigated caspase 1 activity (Fig. 7) and significantly decreased IL-1β in Aβ-stimulated astrocytes examined by ELISA (Fig. 9c, d). Further, there is a trend towards a decrease of IL-1β-protein levels in the presence of MCC950 in nearly all treatment groups,
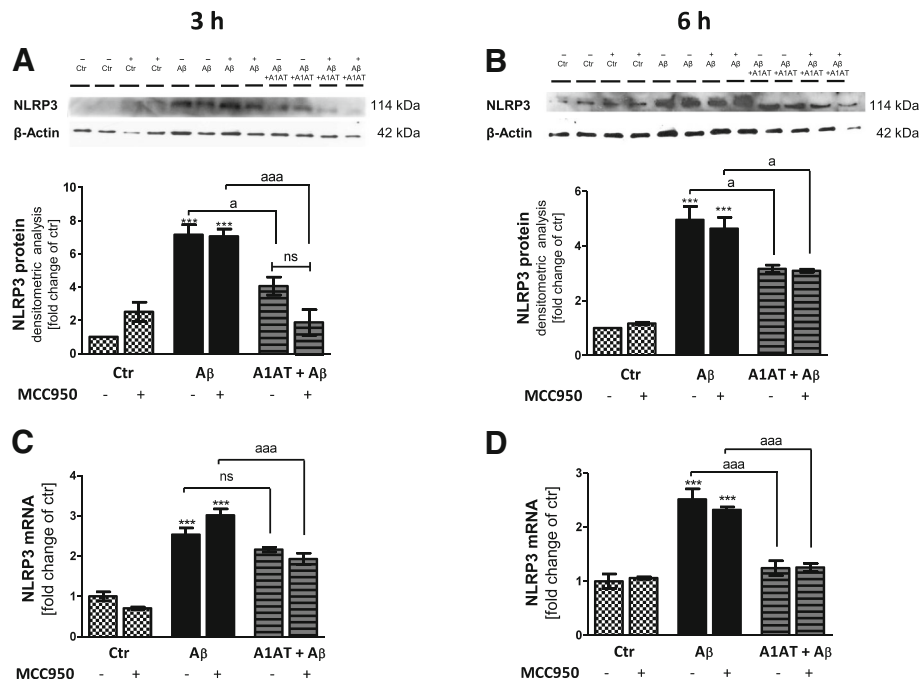
Ebrahimi et al. Journal of Neuroinflammation (2018) 15:282

Page 9 of 15

Fig. 4 Treatment with A1AT abrogated Aβ$_{1-42}$-induced upregulation of NLRP3 mRNA and protein in primary astrocytes. Western blot confirmed an Aβ$_{1-42}$-induced significant increase of NLRP3 protein levels at 3 h (**a**) and 6 h (**b**). Co-treatment with A1AT significantly attenuated this increase at 3 h (**a**) and 6 h (**b**) stimulation time. Addition of MCC950 did not alter NLRP3-protein levels in all treatment groups. Treatment with Aβ$_{1-42}$ significantly increased mRNA levels of NLRP3 in astrocytes at 3 h (**c**) and 6 h (**d**). Co-treatment with A1AT significantly blocked this increase in NLRP3 mRNA expression. MCC950-pretreatment had no effects on NLRP3 mRNA expression at 3 h and 6 h. Data of $n = 3$ in triplicate represent mean ± SD. $*/^{a}p < 0.05$; $**/^{aa}p < 0.01$; $***/^{aaa}p < 0.001$, ns not significant compared to untreated cell control (ctr)
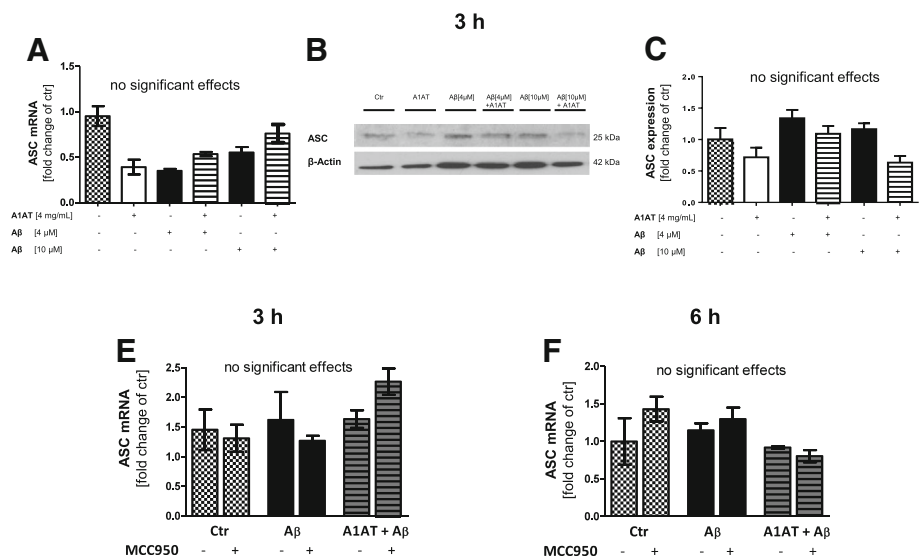

Fig. 5 ASC was not regulated by Aβ$_{1-42}$ and A1AT at 3 h and 6 h stimulation. (**a**) Quantitative RT-PCR demonstrated ASC was not regulated by Aβ$_{1-42}$ or A1AT. Data of $n = 6$ in triplicate represent mean ± SD. (**b-c**) Western blot revealed no regulation of ASC by Aβ$_{1-42}$ or A1AT. Data of $n = 3$ in triplicate represent mean ± SD. (**e-f**) RT-PCR demonstrated that also at 6 h stimulation time such as MCC950-pretreatment did not regulate ASC mRNA expression. Data of $n = 3$ in triplicate represent mean ± SD. $*/^{a}p < 0.05$; $**/^{aa}p < 0.01$; $***/^{aaa}p < 0.001$, ns not significant compared to untreated cell control (ctr)

Ebrahimi *et al. Journal of Neuroinflammation* (2018) 15:282
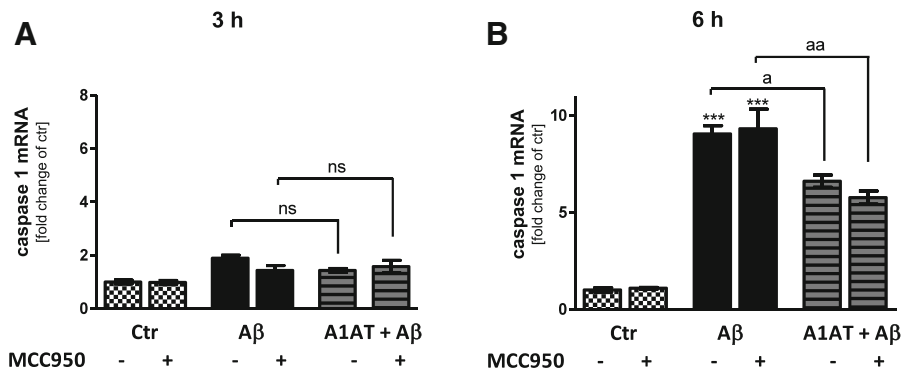
Page 10 of 15

Fig. 6 A1AT time-dependently blocked Aβ$_{1-42}$-induced upregulation of caspase 1 mRNA in primary astrocytes. (**b–c**) As quantified by RT-PCR treatment with 4 μM Aβ$_{1-42}$ significantly increased mRNA levels of caspase 1 in astrocytes at 6 h, but not at 3 h. Co-treatment with A1AT blocked this increase in caspase 1 mRNA expression significantly at 6 h, but not at 3 h. Addition of MCC950 had no effects on caspase 1 mRNA expression at both stimulation times. Data of $n = 3$ in triplicate represent mean ± SD.$^{*/a}p < 0.05$; $^{**/aa}p < 0.01$; $^{***/aaa}p < 0.001$, ns not significant compared to untreated cell control (ctr)
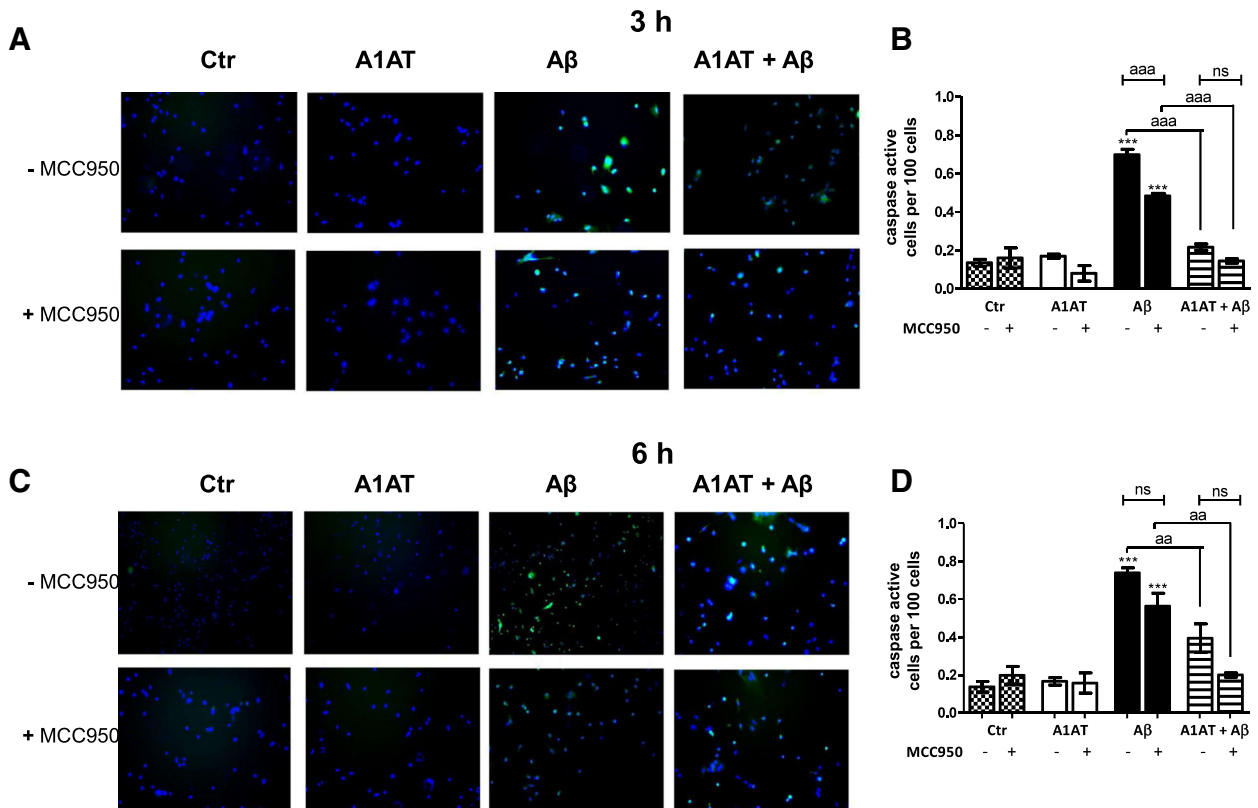

Fig. 7 A1AT mitigated caspase activity in Aβ$_{1-42}$-stimulated astrocytes. (**a, c**) For convenience, we have only illustrated the overlay images of all treatment groups ± MCC950. Counting of caspase active cells (**b, d**) revealed a significant increase of caspase active cells with 4 μM Aβ$_{1-42}$-stimulation at both stimulation times. Co-treatment with A1AT significantly blocked this effect at both stimulation times. In MCC950-treated and Aβ$_{1-42}$-stimulated cells caspase activity significantly declined at 3 h. Additive treatment by MCC950 to A1AT and Aβ$_{1-42}$-stimulated astrocytes did not significantly change caspase activity. Data of $n = 3$ in triplicate represent mean ± SD. $^{*/a}p < 0.05$; $^{**/aa}p < 0.01$; $^{***/aaa}p < 0.001$, ns not significant compared to untreated cell control (ctr)
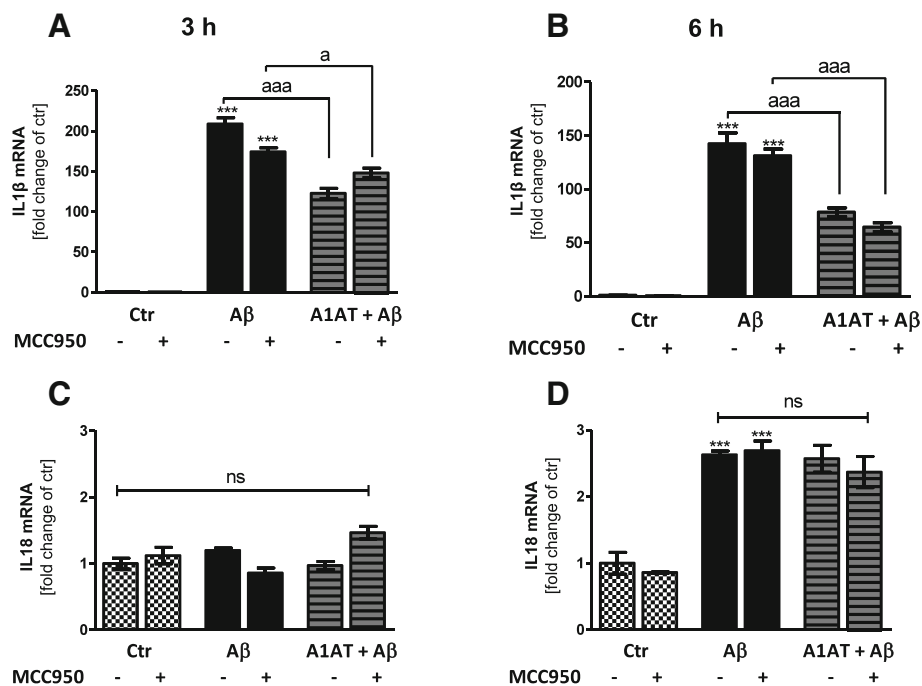
Ebrahimi et al. Journal of Neuroinflammation (2018) 15:282

Page 11 of 15

Fig. 8 A1AT mitigated $A\beta_{1-42}$-induced upregulation of IL-1β mRNA in primary astrocytes. (**a–b**) As quantified by RT-PCR stimulation with 4 μM $A\beta_{1-42}$ significantly increased mRNA levels of IL-1β in astrocytes at 3 h and 6 h. Co-treatment with A1AT blocked this increase significantly at 3 h and 6 h. Addition of MCC950 had no significant impact on gene expression at 3 h and 6 h. (**c**) $A\beta_{1-42}$-stimulation such as A1AT-treatment did not affect IL-18 mRNA expression at 3 h. (**d**) Stimulation with $A\beta_{1-42}$ significantly increased mRNA levels of IL-18 in astrocytes at 6 h. Co-treatment with A1AT did not block this increase. MCC950 had no effects on gene expression of IL-18 at 3 h and 6 h. Data of $n = 3$ in triplicate represent mean ± SD. $*/^a p < 0.05$; $**/^{aa} p < 0.01$; $***/^{aaa} p < 0.001$, ns not significant compared to untreated cell control (ctr)

though not significant (Fig. 9c, d). MCC950 did not affect Aβ-induced expression of IL-1β-precursor protein in western blot (Fig. 9a, b).
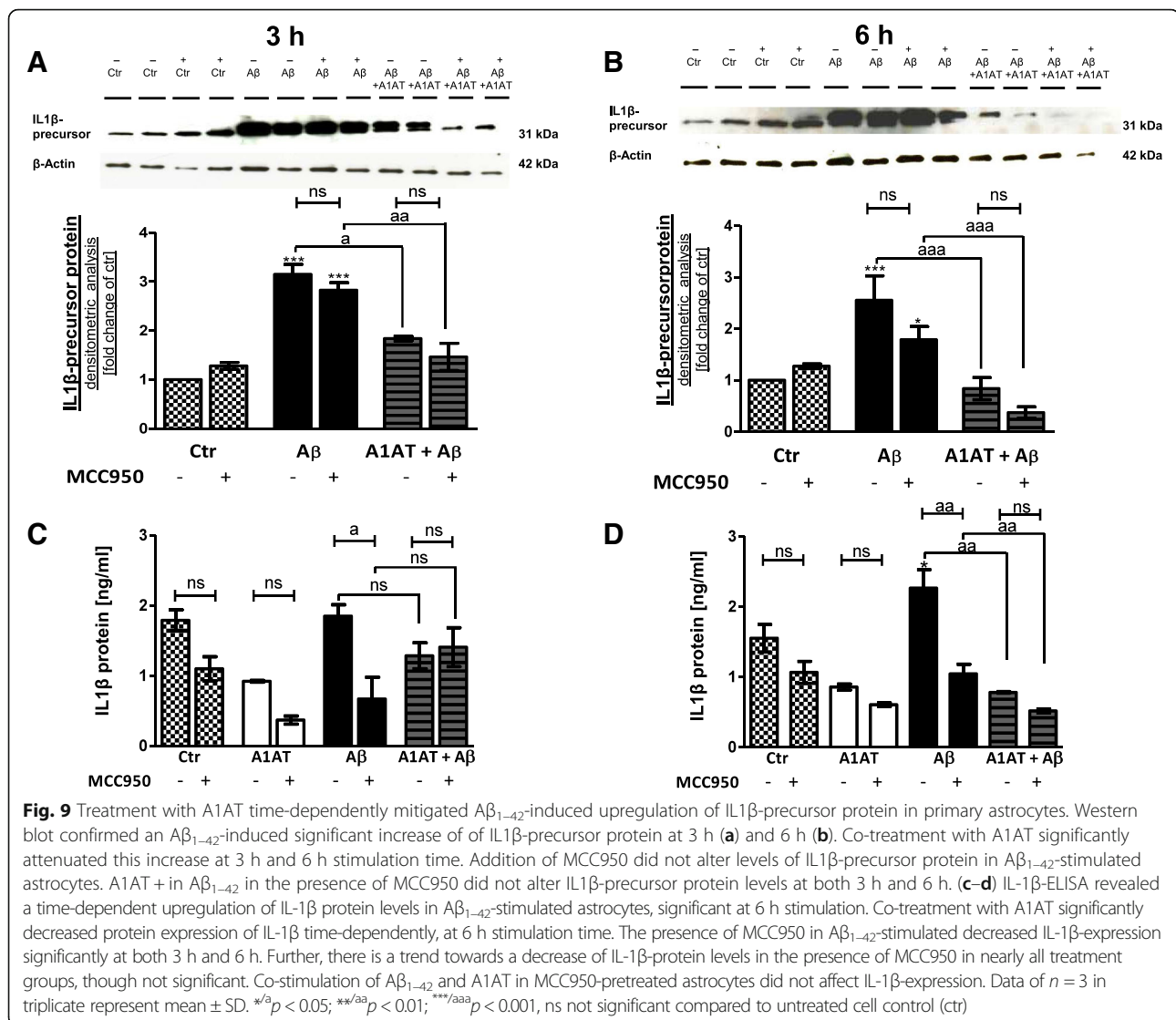
Co-treatment with A1AT and Aβ in the presence of MCC950 did not alter expression of NLRP3-inflammasome components
Examined by caspase 1 assay (Fig. 7), IL-1β western blot (Fig. 9a, b) and IL-1β-ELISA (Fig. 9c, d) co-treatment with A1AT and Aβ in the presence of MCC950 did not alter expression of inflammasome components compared to the same stimulation group in absence of MCC950. Therefore, we conclude that A1AT mitigated IL-1β mainly by inhibiting NLRP3-inflammasome.

Discussion
Activation of glia cells and overexpression of pro-inflammatory cytokines are regarded early events in Alzheimer's disease [56]. In recent years, astrocytes have come into focus in neurodegenerative disorders such as AD and are seen in a new way. Astrocytes express a plethora of receptors and modulate cells and their function in their surroundings [57]. In brief, they are involved in excitotoxic glutamate release, secretion of pro-inflammatory cytokines, growth factor production, stabilization, and organization of the blood-brain barrier

and $A\beta_{1-42}$ production [58]. In microglia cells, the activation of NLRP3 appears to be an essential step during AD. Following activation of NLRP3, inflammation is triggered by the activation of caspase 1 and generation of IL-1β. This hampers the phagocytic capability of microglia cells [39]. The NLRP3-inflammasome is important for the initiation and processing of neuroinflammatory processes, and especially in AD, NLRP3 is associated with age-related inflammation [59]. NLRP3 is known to be activated by $A\beta_{1-42}$-aggregates [14]. NLRP3 knock-out in transgenic animals carrying mutations associated with AD prevents AD pathology [24].

Our group has recently presented data in acute and chronic neurodegenerative disease models that different components of the NLRP3-inflammasome are allocated to astrocytes [60–64]. With respect to AD, Couturier and co-workers were able to show that astrocytes produce and release IL-1β following $A\beta_{1-42}$-stimulation [18]. In this animal model, the downregulation of NLRP3-inflammasome activation leads to decreased amyloid plaques and a better memory performance [35]. Our data now show that stimulation of primary astrocytes with $A\beta_{1-42}$ induces a dose-dependent upregulation of NLRP3. This in turn is known to stimulate the activation of caspase 1 and IL-1β [39]. Our work further demonstrates that such an effect

Ebrahimi *et al. Journal of Neuroinflammation* (2018) 15:282

Page 12 of 15

Fig. 9 Treatment with A1AT time-dependently mitigated $A\beta_{1-42}$-induced upregulation of IL1β-precursor protein in primary astrocytes. Western blot confirmed an $A\beta_{1-42}$-induced significant increase of of IL1β-precursor protein at 3 h (**a**) and 6 h (**b**). Co-treatment with A1AT significantly attenuated this increase at 3 h and 6 h stimulation time. Addition of MCC950 did not alter levels of IL1β-precursor protein in $A\beta_{1-42}$-stimulated astrocytes. A1AT + in $A\beta_{1-42}$ in the presence of MCC950 did not alter IL1β-precursor protein levels at both 3 h and 6 h. (**c–d**) IL-1β-ELISA revealed a time-dependent upregulation of IL-1β protein levels in $A\beta_{1-42}$-stimulated astrocytes, significant at 6 h stimulation. Co-treatment with A1AT significantly decreased protein expression of IL-1β time-dependently, at 6 h stimulation time. The presence of MCC950 in $A\beta_{1-42}$-stimulated decreased IL-1β-expression significantly at both 3 h and 6 h. Further, there is a trend towards a decrease of IL-1β-protein levels in the presence of MCC950 in nearly all treatment groups, though not significant. Co-stimulation of $A\beta_{1-42}$ and A1AT in MCC950-pretreated astrocytes did not affect IL-1β-expression. Data of $n = 3$ in triplicate represent mean ± SD. *[*/a]$p < 0.05$; **[**/aa]$p < 0.01$; ***[***/aaa]$p < 0.001$, ns not significant compared to untreated cell control (ctr)

also occurs after short-term stimulation with $A\beta_{1-42}$. In contrast, the co-treatment of astrocytes with $A\beta_{1-42}$ and A1AT blocks the induction of NLRP3. The regulation of NLRP3 is complex and usually requires a two-step activation process [22]. Currently, it is well accepted that the first step includes a priming signal, usually provided by NF-KB signaling or secretion of endogenous cytokines such as IL-1a [65]. NLRP3 is then activated by a variety of cellular signals, amongst them are misfolded proteins. The large variety of possible regulatory signals and pathways suggest that the activation is rather the consequence of a disturbance of cellular equilibrium [22]. In 2012, Lee and co-workers have identified calcium signaling as essential in NLRP3 activation [66]. In this study, increased intracellular calcium levels are associated with NLRP3 activation. In astrocytes, $A\beta_{1-42}$ potentiates calcium signaling which is triggered by mGlu, α7nAChR, and purinergic substances [57].

Yet, there is little evidence on the regulation of the NLRP3-inflammasome by A1AT. Toldo et al. 2011 stated that A1AT inhibits caspase-1 [67]. Aggarwal et al. 2016 found that—by the presence of polyunsaturated fatty acids—A1AT downregulates NLRP3 and caspase 1 [68]. For astrocytes, no data exist with respect to mechanisms of action of A1AT. In previous studies, we have presented data which show that A1AT reduces inflammation in microglia cells mainly by controlling calcium signaling pathways [15]. A1AT has no effect on classic signaling pathways such as MAPK p38, p44/42, JNK, and cAMP-coupled mechanisms [15]. Using a fluorescent calcium dye, we have shown that A1AT reduces intracellular calcium concentrations in a microglial cell line [15]. A1AT had no direct effect on $A\beta_{1-42}$-oligomerization [15]. We therefore hypothesize that A1AT effects on NLRP3 upregulation in primary astrocytes are mainly triggered by an inhibition of calcium and calpain. This hypothesis

Ebrahimi *et al. Journal of Neuroinflammation* (2018) 15:282

Page 13 of 15

needs further evaluation, since other reports also demonstrate that A1AT is able to reduce glutamate-induced toxicity in murine primary neurons [45]. Since astrocytes release glutamate in response to $A\beta_{1-42}$-stimulation, this could represent another way how A1AT prevents deleterious $A\beta_{1-42}$-induced inflammatory cascades in microglia, neurons, and astrocytes. However, our current study does not include research on how A1AT could regulate the NLRP3-inflammasome complex. Further, it must be remarked that microglia might have partially contributed to the observed results due to the slight contamination of approximately 5%.

Our data demonstrate that NLRP3-inflammasome components are upregulated time-dependently following $A\beta_{1-42}$-stimulation. This can be blocked by A1AT application. NLRP3 is the sensor protein of the NLRP3-inflammasome complex, which explains its upregulation after $A\beta_{1-42}$-stimulation. ASC, in contrast, has the caspase activating and recruitment domain. In our experiments, ASC concentration on the mRNA and protein level was unchanged, indicating that $A\beta_{1-42}$ and A1AT mainly regulate NLRP3, but not ASC. We assume the total amount of ASC to be sufficient to lead to the NLRP3-ASC-complex formation and caspase 1 binding.

To further investigate the direct effect of A1AT on inflammasome-dependent IL-1β maturation, we used a specific NLRP3-inhibitor called MCC950. As previously shown by Coll et al., pre-treatment with MCC950 prevents complex formation of apoptosis-associated speck-like protein containing a CARD (ASC) and blocks the release of IL-1β in immunological active cells, without affecting priming of NLRP3 [46]. Furthermore, MCC950 stimulated Aβ phagocytosis in vitro, and it reduced Aβ accumulation in a mouse model of AD, which was associated with improved cognitive function [50]. In our studies, MCC950-pretreatment in cells co-treated with A1AT and Aβ did not further drop IL-1β protein expression. Thus, A1AT had no effect on protein expression, when NLRP3 was selectively blocked. We therefore conclude that A1AT reduces IL-1β by inhibiting NLRP3-inflammasome.

These observations not only clearly highlight the importance of astroglial-related pro-inflammatory processes in the brain and in particular during AD, but also point at A1AT as a potent antagonist in astrocyte-dependent inflammatory signaling.

Conclusion

We demonstrate that $A\beta_{1-42}$-stimulation results in an upregulation of NLRP3, caspase 1, and its cleavage products in astrocytes. A1AT time-dependently hampers $A\beta_{1-42}$-triggered neuroinflammation by attenuating NLRP3-inflammasome expression. This suggests that A1AT offers a therapeutic opportunity for AD treatment.

Additional files

Additional file 1: Figure S2. Cell counting revealed 95.2% astrocytes and 4.5% microglia. Approximately 0.4% of the cells remained undefined. $n = 12$. (PDF 336 kb)

Additional file 2: Figure S1. There are no oligodendrocytes contaminating the cell culture. Non-specific binding of Olig2 on astrocytes was observed. (PDF 316 kb)

Additional file 3: Figure S3. (A) Stimulation with $A\beta_{1-42}$ led to a concentration-dependent LDH-release. For further experiments, $A\beta_{1-42}$ (10 μM) was selected as the maximum concentration to not exceed 50% of cell death. (B) Ascending concentrations of A1AT did not affect cell viability. (C) Co-treatment with $A\beta_{1-42}$ and A1AT did not affect LDH-release, whereas LPS significantly increased LDH-release. Treatment with A1AT significantly reduced LDH-release in LPS-stimulated astrocytes. Data of $n = 6$ in triplicate represent mean ± SD. *$^{/a}p < 0.05$; **$^{/aa}p < 0.01$; ***$^{/aaa}p < 0.001$, ns not significant compared control. (PDF 246 kb)

Additional file 4: Figure S4. No significant differences in cell metabolism were detected after increasing concentrations of $A\beta_{1-42}$ (A), A1AT (B) or co-treatment of A1AT, $A\beta_{1-42}$ and LPS (C). Data of $n = 6$ in triplicate represent mean ± SD, ns not significant compared to control. (PDF 260 kb)

Additional file 5: Figure S5. (A) Since there are no oligodendrocytes contaminating the cell culture, NLRP3-expression was not oligodendrocyte-induced. (B) NLRP3-expression was indeed induced by the few present microglia. But the majority of NLRP3-expression was not microglia-mediated. $n = 3$. (PDF 385 kb)

Additional file 6: Figure S6. (A) 10 μM $A\beta_{1-42}$ significantly increased caspase 1 mRNA. Co-treatment with A1AT blocked the increase of caspase 1 mRNA expression significantly. (B) Stimulation with $A\beta_{1-42}$ significantly increased IL-1β mRNA. Gene expression of IL-1β was significantly reduced with A1AT-co-treatment. (C) In contrast, $A\beta_{1-42}$-stimulation such as A1AT-treatment did not affect IL-18 mRNA expression. Data of $n = 6$ in triplicate represent mean ± SD. *$^{/a}p < 0.05$; **$^{/aa}p < 0.01$; ***$^{/aaa}p < 0.001$ compared to control. (PDF 238 kb)

Abbreviations
A1AT: α1-antitrypsin; AD: Alzheimer's disease; ASC: Apoptosis-associated speck-like protein containing a CARD; Aβ: Amyloid β; CARD: Caspase activation and recruitment domain; Casp1: Caspase 1; CNS: Central nervous system; Ctr: Control; DMSO: Dimethylsulfoxid; GAPDH: Glycerinaldehyd-3-phosphate-dehydrogenase; GFAP: Glial fibrillary acidic protein; HPRT: Hypoxanthine phosphoribosyltransferase; Hsp90: Heat shock protein 90; Iba1: Ionized calcium binding adaptor molecule 1; ICC: Immunocytochemistry; IL-18: Interleukin-18; IL-1β: Interleukin-1β; LDH: Lactate dehydrogenase; LPS: Lipopolysaccharide; LRR: Leucine-rich repeat; NACHT: NAIP (NLP family apoptosis inhibitor protein), CIITA (class 2 transcription activator), HET-E (heterokaryon incompatibility), TEP1 (telomerase-associated protein 1); NLRP: NACHT, LRR, and PYD domains-containing; PCR: Polymerase chain reaction; Pos: Positive control; PYD: Pyrin domain; q-RT-PCR: Quantitative real-time PCR; RFU: Relative fluorescence units; sq-PCR: Semi-quantitative PCR

Availability of data and materials
All data generated or analyzed during this study are included in this published article and its supplementary information files.

Authors' contributions
JPB and PH conceived the conceptual idea, coordinated and designed the study, and corrected the manuscript. JPB and PH planned and supervised the experiments. TE conducted the experiments and drafted the manuscript. AS, PH, and TE performed the preparation of cells. MR assisted in the conduction of the experiments. TE, SNK, and AS carried out the western

blots. AS and PH performed the statistical analysis. JPB, PH, and TE interpreted the results. CB, ARK, and JBS revised the manuscript and provided critical feedback. All authors read and approved the final manuscript.

Publisher's Note

Author details
[1]Department of Neurology, RWTH Aachen University, Aachen, Germany.
[2]Institute of Neuroanatomy, RWTH Aachen University, Aachen, Germany.
[3]Department of Internal Medicine, Pulmonary and Critical Care Medicine, University Medical Center Giessen and Marburg, Marburg, Germany.
[4]JARA-Institute Molecular Neuroscience and Neuroimaging, Forschungszentrum Jülich GmbH and RWTH Aachen University, Aachen, Germany.

References
1. Prince M, Bryce R, Albanese E, Wimo A, Ribeiro W, Ferri CP. The global prevalence of dementia: a systematic review and metaanalysis. Alzheimers Dement. 2013;9(1):63–75.e62.
2. Brookmeyer R, Johnson E, Ziegler-Graham K, Arrighi HM. Forecasting the global burden of Alzheimer's disease. Alzheimers Dement. 2007;3(3):186–91.
3. Hirtz D, Thurman DJ, Gwinn-Hardy K, Mohamed M, Chaudhuri AR, Zalutsky R. How common are the "common" neurologic disorders? Neurology. 2007; 68(5):326–37.
4. Rosenberg PB, Lyketsos C. Mild cognitive impairment: searching for the prodrome of Alzheimer's disease. World Psychiatry. 2008;7(2):72–8.
5. Wilson RS, Leurgans SE, Boyle PA, Bennett DA. Cognitive decline in prodromal Alzheimer disease and mild cognitive impairment. Arch Neurol. 2011;68(3):351–6.
6. Ringman JM, Liang LJ, Zhou Y, Vangala S, Teng E, Kremen S, Wharton D, Goate A, Marcus DS, Farlow M, et al. Early behavioural changes in familial Alzheimer's disease in the dominantly inherited Alzheimer network. Brain. 2015;138(Pt 4):1036–45.
7. Bature F, Guinn BA, Pang D, Pappas Y. Signs and symptoms preceding the diagnosis of Alzheimer's disease: a systematic scoping review of literature from 1937 to 2016. BMJ Open. 2017;7(8):e015746.
8. Hsu D, Marshall GA. Primary and secondary prevention trials in Alzheimer disease: looking back, Moving Forward. Curr Alzheimer Res. 2017;14(4):426–40.
9. Karakaya T, Fusser F, Schroder J, Pantel J. Pharmacological treatment of mild cognitive impairment as a prodromal syndrome of Alzheimer's disease. Curr Neuropharmacol. 2013;11(1):102–8.
10. Dubois B, Zaim M, Touchon J, Vellas B, Robert P, Murphy MF, Pujadas-Navines F, Rainer M, Soininen H, Riordan HJ, et al. Effect of six months of treatment with V0191 in patients with suspected prodromal Alzheimer's disease. J Alzheimers Dis. 2012;29(3):527–35.
11. Caldwell CC, Yao J, Brinton RD. Targeting the prodromal stage of Alzheimer's disease: bioenergetic and mitochondrial opportunities. Neurotherapeutics. 2015;12(1):66–80.
12. Haass C, Selkoe DJ. Soluble protein oligomers in neurodegeneration: lessons from the Alzheimer's amyloid beta-peptide. Nat Rev Mol Cell Biol. 2007;8(2):101–12.
13. Baglioni S, Casamenti F, Bucciantini M, Luheshi LM, Taddei N, Chiti F, Dobson CM, Stefani M. Prefibrillar amyloid aggregates could be generic toxins in higher organisms. J Neurosci. 2006;26(31):8160–7.
14. Halle A, Hornung V, Petzold GC, Stewart CR, Monks BG, Reinheckel T, Fitzgerald KA, Latz E, Moore KJ, Golenbock DT. The NALP3 inflammasome is involved in the innate immune response to amyloid-beta. Nat Immunol. 2008;9(8):857–65.
15. Gold M, Dolga AM, Koepke J, Mengel D, Culmsee C, Dodel R, Koczulla AR, Bach JP. alpha1-antitrypsin modulates microglial-mediated neuroinflammation and protects microglial cells from amyloid-beta-induced toxicity. J Neuroinflammation. 2014;11:165.
16. Saresella M, La Rosa F, Piancone F, Zoppis M, Marventano I, Calabrese E, Rainone V, Nemni R, Mancuso R, Clerici M. The NLRP3 and NLRP1 inflammasomes are activated in Alzheimer's disease. Mol Neurodegener. 2016;11:23.
17. Glass CK, Saijo K, Winner B, Marchetto MC, Gage FH. Mechanisms underlying inflammation in neurodegeneration. Cell. 2010;140(6):918–34.
18. Kraft AD, Harry GJ. Features of microglia and neuroinflammation relevant to environmental exposure and neurotoxicity. Int J Environ Res Public Health. 2011;8(7):2980–3018.
19. Rama Rao KV, Kielian T. Neuron-astrocyte interactions in neurodegenerative diseases: role of neuroinflammation. Clin Exp Neuroimmunol. 2015;6(3):245–63.
20. Goedert M, Wischik CM, Crowther RA, Walker JE, Klug A. Cloning and sequencing of the cDNA encoding a core protein of the paired helical filament of Alzheimer disease: identification as the microtubule-associated protein tau. Proc Natl Acad Sci U S A. 1988;85(11):4051–5.
21. Goedert M, Spillantini MG, Jakes R, Rutherford D, Crowther RA. Multiple isoforms of human microtubule-associated protein tau: sequences and localization in neurofibrillary tangles of Alzheimer's disease. Neuron. 1989;3(4):519–26.
22. Song L, Pei L, Yao S, Wu Y, Shang Y. NLRP3 Inflammasome in neurological diseases, from functions to therapies. Front Cell Neurosci. 2017;11:63.
23. Agostini L, Martinon F, Burns K, McDermott MF, Hawkins PN, Tschopp J. NALP3 forms an IL-1beta-processing inflammasome with increased activity in Muckle-Wells autoinflammatory disorder. Immunity. 2004;20(3):319–25.
24. Heneka MT, Kummer MP, Stutz A, Delekate A, Schwartz S, Vieira-Saecker A, Griep A, Axt D, Remus A, Tzeng TC, et al. NLRP3 is activated in Alzheimer's disease and contributes to pathology in APP/PS1 mice. Nature. 2013; 493(7434):674–8.
25. Sutterwala FS, Haasken S, Cassel SL. Mechanism of NLRP3 inflammasome activation. Ann N Y Acad Sci. 2014;1319:82–95.
26. Martinon F. Detection of immune danger signals by NALP3. J Leukoc Biol. 2008;83(3):507–11.
27. Martinon F, Burns K, Tschopp J. The inflammasome: a molecular platform triggering activation of inflammatory caspases and processing of proIL-beta. Mol Cell. 2002;10(2):417–26.
28. Yatsiv I, Morganti-Kossmann MC, Perez D, Dinarello CA, Novick D, Rubinstein M, Otto VI, Rancan M, Kossmann T, Redaelli CA, et al. Elevated intracranial IL-18 in humans and mice after traumatic brain injury and evidence of neuroprotective effects of IL-18-binding protein after experimental closed head injury. J Cereb Blood Flow Metab. 2002;22(8):971–8.
29. Merrill JE, Benveniste EN. Cytokines in inflammatory brain lesions: helpful and harmful. Trends Neurosci. 1996;19(8):331–8.
30. Codolo G, Plotegher N, Pozzobon T, Brucale M, Tessari I, Bubacco L, de Bernard M. Triggering of inflammasome by aggregated alpha-synuclein, an inflammatory response in synucleinopathies. PLoS One. 2013;8(1):e55375.
31. Mao Z, Liu C, Ji S, Yang Q, Ye H, Han H, Xue Z. The NLRP3 Inflammasome is involved in the pathogenesis of Parkinson's disease in rats. Neurochem Res. 2017;42(4):1104–15.
32. Zhou Y, Lu M, Du RH, Qiao C, Jiang CY, Zhang KZ, Ding JH, Hu G. MicroRNA-7 targets nod-like receptor protein 3 inflammasome to modulate neuroinflammation in the pathogenesis of Parkinson's disease. Mol Neurodegener. 2016;11:28.
33. Zhang P, Shao XY, Qi GJ, Chen Q, Bu LL, Chen LJ, Shi J, Ming J, Tian B. Cdk5-dependent activation of neuronal Inflammasomes in Parkinson's disease. Mov Disord. 2016;31(3):366–76.
34. Yang F, Wang Z, Wei X, Han H, Meng X, Zhang Y, Shi W, Li F, Xin T, Pang Q, et al. NLRP3 deficiency ameliorates neurovascular damage in experimental ischemic stroke. J Cereb Blood Flow Metab. 2014;34(4):660–7.
35. Couturier J, Stancu IC, Schakman O, Pierrot N, Huaux F, Kienlen-Campard P, Dewachter I, Octave JN. Activation of phagocytic activity in astrocytes by reduced expression of the inflammasome component ASC and its implication in a mouse model of Alzheimer disease. J Neuroinflammation. 2016;13:20.
36. Dong Y, Benveniste EN. Immune function of astrocytes. Glia. 2001;36(2):180–90.

Ebrahimi *et al. Journal of Neuroinflammation* (2018) 15:282

Page 15 of 15

37. Akiyama H, Arai T, Kondo H, Tanno E, Haga C, Ikeda K. Cell mediators of inflammation in the Alzheimer disease brain. Alzheimer Dis Assoc Disord. 2000;14(Suppl 1):S47–53.

38. Salminen A, Ojala J, Suuronen T, Kaarniranta K, Kauppinen A. Amyloid-beta oligomers set fire to inflammasomes and induce Alzheimer's pathology. J Cell Mol Med. 2008;12(6A):2255–62.

39. Gold M, El Khoury J. beta-amyloid, microglia, and the inflammasome in Alzheimer's disease. Semin Immunopathol. 2015;37(6):607–11.

40. Freeman L, Guo H, David CN, Brickey WJ, Jha S, Ting JP. NLR members NLRC4 and NLRP3 mediate sterile inflammasome activation in microglia and astrocytes. J Exp Med. 2017;214(5):1351–70.

41. Tumen J, Meyrick B, Berry L Jr, Brigham KL. Antiproteinases protect cultured lung endothelial cells from endotoxin injury. J Appl Physiol (1985). 1988; 65(2):835–43.

42. Libert C, Van Molle W, Brouckaert P, Fiers W. alpha1-Antitrypsin inhibits the lethal response to TNF in mice. J Immunol. 1996;157(11):5126–9.

43. Van Molle W, Libert C, Fiers W, Brouckaert P. Alpha 1-acid glycoprotein and alpha 1-antitrypsin inhibit TNF-induced but not anti-Fas-induced apoptosis of hepatocytes in mice. J Immunol. 1997;159(7):3555–64.

44. Janciauskiene S, Larsson S, Larsson P, Virtala R, Jansson L, Stevens T. Inhibition of lipopolysaccharide-mediated human monocyte activation, in vitro, by alpha1-antitrypsin. Biochem Biophys Res Commun. 2004;321(3):592–600.

45. Gold M, Koczulla AR, Mengel D, Koepke J, Dodel R, Dontcheva G, Habib P, Bach JP. Reduction of glutamate-induced excitotoxicity in murine primary neurons involving calpain inhibition. J Neurol Sci. 2015;359(1–2):356–62.

46. Coll RC, Robertson AA, Chae JJ, Higgins SC, Munoz-Planillo R, Inserra MC, Vetter I, Dungan LS, Monks BG, Stutz A, et al. A small-molecule inhibitor of the NLRP3 inflammasome for the treatment of inflammatory diseases. Nat Med. 2015;21(3):248–55.

47. Levy M, Thaiss CA, Elinav E. Taming the inflammasome. Nat Med. 2015;21(3):213–5.

48. Ismael S, Nasoohi S, Ishrat T. MCC950, the selective inhibitor of nucleotide oligomerization domain-like receptor Protein-3 inflammasome, protects mice against traumatic brain injury. J Neurotrauma. 2018;35(11):1294–303.

49. Perera AP, Fernando R, Shinde T, Gundamaraju R, Southam B, Sohal SS, Robertson AAB, Schroder K, Kunde D, Eri R. MCC950, a specific small molecule inhibitor of NLRP3 inflammasome attenuates colonic inflammation in spontaneous colitis mice. Sci Rep. 2018;8(1):8618.

50. Dempsey C, Rubio Araiz A, Bryson KJ, Finucane O, Larkin C, Mills EL, Robertson AAB, Cooper MA, O'Neill LAJ, Lynch MA. Inhibiting the NLRP3 inflammasome with MCC950 promotes non-phlogistic clearance of amyloid-beta and cognitive function in APP/PS1 mice. Brain Behav Immun. 2017;61:306–16.

51. Habib P, Dang J, Slowik A, Victor M, Beyer C. Hypoxia-induced gene expression of aquaporin-4, cyclooxygenase-2 and hypoxia-inducible factor 1alpha in rat cortical astroglia is inhibited by 17beta-estradiol and progesterone. Neuroendocrinology. 2014;99(3–4):156–67.

52. Kayed R, Head E, Thompson JL, McIntire TM, Milton SC, Cotman CW, Glabe CG. Common structure of soluble amyloid oligomers implies common mechanism of pathogenesis. Science. 2003;300(5618):486–9.

53. Habib P, Dreymueller D, Ludwig A, Beyer C, Dang J. Sex steroid hormone-mediated functional regulation of microglia-like BV-2 cells during hypoxia. J Steroid Biochem Mol Biol. 2013;138:195–205.

54. Dang J, Mitkari B, Kipp M, Beyer C. Gonadal steroids prevent cell damage and stimulate behavioral recovery after transient middle cerebral artery occlusion in male and female rats. Brain Behav Immun. 2011;25(4):715–26.

55. Johann S, Dahm M, Kipp M, Zahn U, Beyer C. Regulation of choline acetyltransferase expression by 17 beta-oestradiol in NSC-34 cells and in the spinal cord. J Neuroendocrinol. 2011;23(9):839–48.

56. Heneka MT, Golenbock DT, Latz E. Innate immunity in Alzheimer's disease. Nat Immunol. 2015;16(3):229–36.

57. Acosta C, Anderson HD, Anderson CM. Astrocyte dysfunction in Alzheimer disease. J Neurosci Res. 2017;95(12):2430–47.

58. Sofroniew MV. Molecular dissection of reactive astrogliosis and glial scar formation. Trends Neurosci. 2009;32(12):638–47.

59. Youm YH, Grant RW, McCabe LR, Albarado DC, Nguyen KY, Ravussin A, Pistell P, Newman S, Carter R, Laque A, et al. Canonical Nlrp3 inflammasome links systemic low-grade inflammation to functional decline in aging. Cell Metab. 2013;18(4):519–32.

60. Johann S, Heitzer M, Kanagaratnam M, Goswami A, Rizo T, Weis J, Troost D, Beyer C. NLRP3 inflammasome is expressed by astrocytes in the SOD1 mouse model of ALS and in human sporadic ALS patients. Glia. 2015;63(12):2260–73.

61. Heitzer M, Kaiser S, Kanagaratnam M, Zendedel A, Hartmann P, Beyer C, Johann S. Administration of 17beta-estradiol improves motoneuron survival and Down-regulates Inflammasome activation in male SOD1(G93A) ALS mice. Mol Neurobiol. 2017;54(10):8429–43.

62. Mortezaee K, Khanlarkhani N, Beyer C, Zendedel A. Inflammasome: its role in traumatic brain and spinal cord injury. J Cell Physiol. 2017;233(7):5160–9.

63. Zendedel A, Monnink F, Hassanzadeh G, Zaminy A, Ansar MM, Habib P, Slowik A, Kipp M, Beyer C. Estrogen attenuates local Inflammasome expression and activation after spinal cord injury. Mol Neurobiol. 2017;55(2):1364–75.

64. Debye B, Schmulling L, Zhou L, Rune G, Beyer C, Johann S. Neurodegeneration and NLRP3 inflammasome expression in the anterior thalamus of SOD1(G93A) ALS mice. Brain Pathol. 2016;28(1):14–27.

65. Bauernfeind FG, Horvath G, Stutz A, Alnemri ES, MacDonald K, Speert D, Fernandes-Alnemri T, Wu J, Monks BG, Fitzgerald KA, et al. Cutting edge: NF-kappaB activating pattern recognition and cytokine receptors license NLRP3 inflammasome activation by regulating NLRP3 expression. J Immunol. 2009;183(2):787–91.

66. Lee GS, Subramanian N, Kim AI, Aksentijevich I, Goldbach-Mansky R, Sacks DB, Germain RN, Kastner DL, Chae JJ. The calcium-sensing receptor regulates the NLRP3 inflammasome through Ca2+ and cAMP. Nature. 2012; 492(7427):123–7.

67. Toldo S, Seropian IM, Mezzaroma E, Van Tassell BW, Salloum FN, Lewis EC, Voelkel N, Dinarello CA, Abbate A. Alpha-1 antitrypsin inhibits caspase-1 and protects from acute myocardial ischemia-reperfusion injury. J Mol Cell Cardiol. 2011;51(2):244–51.

68. Aggarwal N, Korenbaum E, Mahadeva R, Immenschuh S, Grau V, Dinarello CA, Welte T, Janciauskiene S. alpha-Linoleic acid enhances the capacity of alpha-1 antitrypsin to inhibit lipopolysaccharide-induced IL-1beta in human blood neutrophils. Mol Med. 2016;22:680–93.